JACS
JOURNAL OF THE AMERICAN CHEMICAL SOCIETY

ARTICLE

pubs.acs.org/JACS

Probing the Charge-Transfer Dynamics in DNA at the Single-Molecule Level

Kiyohiko Kawai,*,† Eri Matsutani,† Atsushi Maruyama,‡ and Tetsuro Majima*,†

†The Institute of Scientific and Industrial Research (SANKEN), Osaka University, Mihogaoka 8-1, Ibaraki, Osaka 567-0047, Japan
‡Institute for Materials Chemistry and Engineering, Kyushu University, Motooka 744-CE11, Nishi-ku, Fukuoka 819-0395, Japan

Supporting Information

ABSTRACT: Photoinduced charge-transfer fluorescence quenching of a fluorescent dye produces the nonemissive charge-separated state, and subsequent charge recombination makes the reaction reversible. While the information available from the photoinduced charge-transfer process provides the basis for monitoring the microenvironment around the fluorescent dyes and such monitoring is particularly important in live-cell imaging and DNA diagnosis, the information obtainable from the charge recombination process is usually overlooked. When looking at fluorescence emitted from each single fluorescent dye, photoinduced charge-transfer, charge-migration, and charge recombination cause a "blinking" of the fluorescence, in which the charge-recombination rate or the lifetime of the charge-separated state (τ) is supposed to be reflected in the duration of the off time during the single-molecule-level fluorescence measurement. Herein, based on our recently developed method for the direct observation of charge migration in DNA, we utilized DNA as a platform for spectroscopic investigations of charge-recombination dynamics for several fluorescent dyes: TAMRA, ATTO 655, and Alexa 532, which are used in single-molecule fluorescence measurements. Charge recombination dynamics were observed by transient absorption measurements, demonstrating that these fluorescent dyes can be used to monitor the charge-separation and charge-recombination events. Fluorescence correlation spectroscopy (FCS) of ATTO 655 modified DNA allowed the successful measurement of the charge-recombination dynamics in DNA at the single-molecule level. Utilizing the injected charge just like a pulse of sound, such as a "ping" in active sonar systems, information about the DNA sequence surrounding the fluorescent dye was read out by measuring the time it takes for the charge to return.

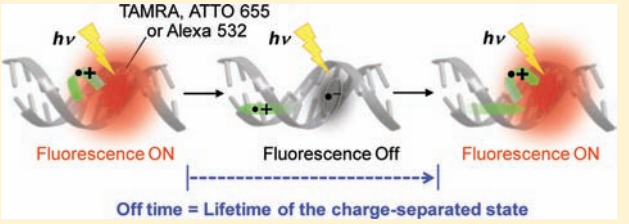

INTRODUCTION

Taking advantage of their relatively small sizes compared with fluorescent proteins and quantum dots, fluorescent dyes are widely used as labeling tools in biological imaging and diagnosis.[1−3] The fluorescence emitted from a fluorescent dye can be modulated by the microenvironment surrounding the fluorescent dye, and photoinduced charge-transfer quenching is one of such mechanisms that causes a fluctuation of the fluorescence emission. Since the fluorescence quenching efficiency or the photoinduced charge-transfer rate is strongly affected by the distance and the intervening medium between the fluorescent dye and the electron-donating biomolecules such as tryptophan in the polypeptide and guanine (G) in the DNA,[2−5] information about the microenvironment around the fluorescent dye can be extracted by measuring the change in either the fluorescence intensity or the fluorescence lifetime.

Photoinduced charge-transfer quenching results in the formation of a nonemissive radical-ion state of the fluorescent dye and charge injection into a biomolecule. An injected charge can migrate along the biomolecule, and subsequent charge-recombination makes the reaction reversible, thereby rendering the fluorescent dye suitable for live-cell imaging and diagnosis. The charge-migration dynamics along the biomolecule are reflected in a change in the charge-recombination rate or the lifetime of the charge separated state (τ); thus, the measurement of τ would provide us with additional unique and fruitful information around the fluorescent dye.[6−21] While the information available from the photoinduced charge transfer rate can be readily accessed by measuring the change in either the fluorescence intensity or the fluorescence lifetime, the τ is usually determined by the transient absorption measurement, which is labor-intensive and requires a significant amount of sample (>1 nmol); thus, the information obtainable from the charge recombination dynamics is usually overlooked during live-cell imaging and diagnosis.

Recent advances in fluorescence microscopy techniques now allow us to trace the fluorescence emitted from each individual fluorescent dye in living cells. Since the photoinduced charge-transfer transforms the fluorescent dye into the nonemissive state, fluorescent dye cannot emit until the charge-recombination takes place. Thus, the photoinduced charge-transfer quenching can cause blinking of the fluorescence during the single-molecule fluorescence measurement, and blinking is often attributed to the

Received: May 26, 2011
Published: August 29, 2011

dx.doi.org/10.1021/ja206325m | J. Am. Chem. Soc. 2011, 133, 15568–15577

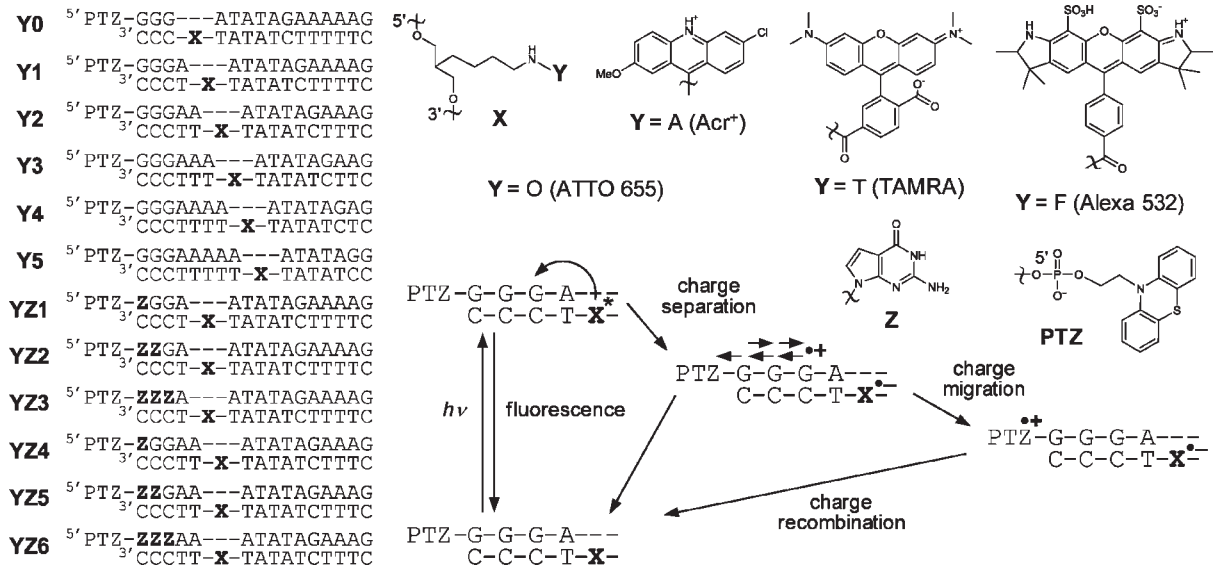

Figure 1. DNA sequences used in this study, chemical structures of an aminolinker (X), Acr^+, TAMRA, Alexa 532 (the structure of ATTO 655 is proprietary), 7-deazaguanine (Z), and a positive charge trap phenothiazine (PTZ), and a schematic representation for charge injection, charge-migration, and charge-recombination in DNA. In the case of Alexa 532 modified DNA, an additional T was placed as a complementary base of X.

formation of the charge-separated state.[22−29] Since the time resolution of current single-molecule fluorescence techniques in living cells is practically limited to a sub-microsecond level,[30,31] contribution of the charge-recombination dynamics in a time range as short as 0.1 μs would be of particular importance during the single-molecule-level fluorescence measurement. However, there have been limited reports regarding the charge-recombination dynamics for the fluorescent dyes used in single-molecule fluorescence measurements.

We have previously reported that charge-separation and -recombination dynamics in DNA can be modulated to have various lifetimes for the charge-separated state in the time range of nanosecond to millisecond by arranging the sequence neighboring the fluorescent dye or a photosensitizer.[19] In this study, we utilized DNA as a platform to investigate the charge-recombination dynamics. Among the four nucleobases, G exhibits the lowest oxidation potential,[4,32,33] and in the case of protonated 9-alkylamino-6-chloro-2-methoxyacridine (Acr^+), the fluorescence of which can only be quenched by G,[34−37] an A−T base-pair serves as a spacer to slow down the charge-recombination rate, allowing for the formation of a long-lived charge-separated state.[20] Thus, fluorescent dyes for which the fluorescence can only be quenched by G would be suitable for the observation of charge-recombination dynamics in DNA. We focused specifically on fluorescent dyes that can only oxidize G upon photoexcitation, and selected TAMRA, ATTO 655, and Alexa 532 as candidates for the observation of charge-recombination dynamics. These fluorescent dyes fulfill the properties required for single-molecule fluorescence measurements such as a high level of brightness, high photostability, and emission in the visible light range. They can maintain a high level of brightness in the context of DNA by properly regulating the distance between the neighboring G's to control the charge-transfer processes, and thus are widely used in fluorescence labeling of DNA and RNA.[38−49] Transient absorption measurements allowed the direct observation of charge-recombination dynamics in fluorescent dye-modified DNA, demonstrating that, similar to Acr^+, TAMRA, ATTO 655, and Alexa 532 undergo charge-separation and recombination in DNA in the time range of nanosecond to milliseconds.

We chose ATTO 655 to probe the charge recombination dynamics in DNA at the single-molecule level. The blinking caused by charge-separation and -recombination dynamics in DNA in the time range of microsecond to tens of microseconds was clearly probed by fluorescence correlation spectroscopy (FCS),[25,47−57] which enabled the read-out of DNA sequence information including data on single-nucleotide polymorphisms (SNPs) at the single-molecule level.

RESULTS AND DISCUSSION

DNA Sequence Design. The photoinduced charge-transfer rate from a fluorescent dye in the singlet excited state to neighboring G exponentially decreases with increasing numbers of intervening A−T base-pairs, as previously reported by Lewis and Wasielewski,[58] Barton and co-workers,[11,59] Michel-Beyerle and co-workers,[34,35] Fukui et al.,[36,37] and by us.[20] Herein, DNAs were designed so as to have between zero and five intervening A−T base-pairs between a fluorescent dye and G (Figure 1). The fluorescent dyes were anchored and buried in DNA to have a π-stacking interaction between neighboring bases by using the amino-linker X. We used phenothiazine (PTZ: E_{ox} = 0.76 V vs NHE)[60] as a positive charge trap having a much lower oxidation potential than G (E_{ox} = 1.31 V vs NHE).[33] Similar to the photoinduced charge-transfer process, the charge-recombination rate, that is, τ also increases with increasing distance between the fluorescent dye and the charge trap. To generate a long-lived charge-separated state, it is important to separate the fluorescent dye and PTZ by a sufficiently long distance.[19,20] We utilized three consecutive G−C base-pairs as a pathway of a positive charge to further separate the positive and negative charge (one-electron reduced fluorescent dye). The initial charge-recombination between the one-electron reduced fluorescent dye and the radical cation of G proceeds relatively fast compared with the

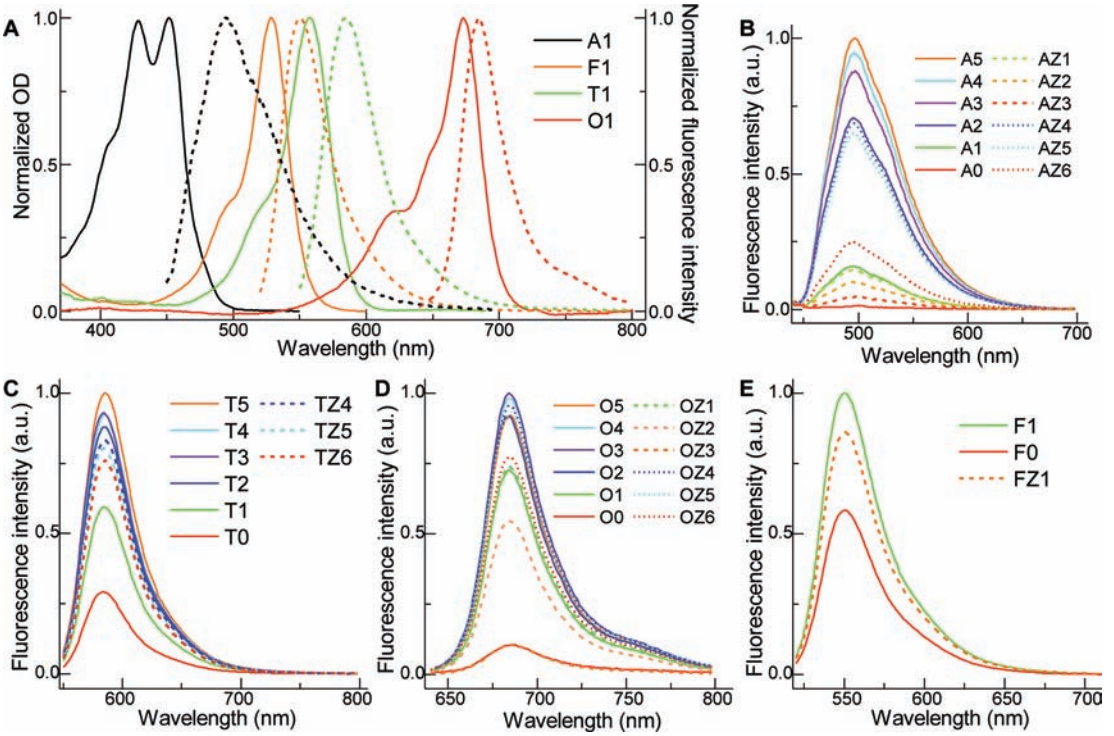

Figure 2. (A) Absorption (bold line) and fluorescence spectra (dashed line) of Acr^+, TAMRA, ATTO 655, and Alexa 532 modified DNA. (B–E) Fluorescence spectra for (B) Acr^+-modified DNA (λ_{ex} = 428 nm), (C) TAMRA-modified DNA (λ_{ex} = 540 nm), (D) ATTO 655-modified DNA (λ_{ex} = 620 nm), and (E) Alexa 532-modified DNA (λ_{ex} = 510 nm).

charge-migration process through DNA, and only part of a generated positive charge can escape from the initial charge recombination to be trapped at PTZ to form a long-lived charge separated state.[20] We also replaced some G's within the consecutive G–C base-pairs with deazaguanine (Z: E_{ox} = 0.98 V vs NHE),[33,59,61,62] which have a lower oxidation potential than G, to refine the charge-separation process to achieve a larger quantum yield of the long-lived charge-separated state (Φ). Consequently, DNAs were synthesized so as to contain a $(A–T)_n$ (n = 0–5) spacer and an $(X–C)_3$ (X = G or Z) charge pathway between the fluorescent dye and PTZ. The incorporation yield for Alexa 532 was low, and thus, only **F0**, **F1**, and **FZ1** were synthesized.

Photoinduced Charge-Transfer Fluorescence Quenching. The steady-state fluorescence spectra were measured to investigate the photoinduced fluorescence quenching. We first tested Acr^+ to verify the present system. Consistent with previous reports by Michel-Beyerle and co-workers,[34,35] Fukui et al.,[36,37] and us,[20] the fluorescence intensity decreased as the number of intervening A–T base-pairs between Acr^+ and G decreased according with the distant-dependent photoinduced charge-transfer between Acr^+ in the singlet-excited state and G (Figure 2B). Similar trends were observed for TAMRA, ATTO 655, and Alexa 532, suggesting the occurrence of photoinduced charge-transfer between the fluorescent dye in the singlet excited state and G (Figure 2C–E). The replacement of G close to the fluorescent dye with Z resulted in a further decrease in the fluorescent intensity due to the more efficient fluorescence quenching by Z compared with G, while changes in the bases far from the fluorescent dye caused only small effects on the fluorescence intensity.

Charge-Recombination Dynamics. The formation of the charge-separated state was characterized by nanosecond time-resolved transient absorption measurements. In the case of Acr^+-modified DNA, Acr^+ was excited using the 355-nm laser, and the charge-recombination dynamics were monitored by formation and decay of $PTZ^{\bullet+}$ and $Acr^{\bullet}$, which show absorption with a peak at around 520 nm (Figure 3A).[20,34,35] When there was no A–T spacer between G and Acr^+, formation of the charge-separated state was not observed because the charge-recombination took place faster than the time resolution of our experimental setup (<50 ns).[20,34,35] The insertion of the A–T base-pair between G and Acr^+ slowed the initial charge-recombination rate between the $Acr^{\bullet}$ and $G^{\bullet+}$, resulting in the formation of a long-lived charge-separated state, and τ increased while Φ gradually decreased with increasing numbers of A–T base-pairs, consistent with previous reports (Figure 3B).[20]

Next, charge-recombination dynamics were investigated for TAMRA, ATTO 655, and Alexa 532 modified DNA. Since the absorption of $PTZ^{\bullet+}$ overlaps with the ground state absorption of these fluorescent dyes and also their absorption spectra in the radical anion form have not been reported thus far, charge-recombination dynamics were investigated by monitoring the bleach and recovery of the ground state absorption of the fluorescent dye. The fluorescence lifetimes of TAMRA,[63] ATTO 655,[42] and Alexa 532[64] are reported to be shorter than 10 ns, and thus would not significantly disturb the observation of the long-lived charge-separated state. The 532-nm laser flash excitation of the TAMRA-modified DNA caused bleach and recovery of the ground state absorption of TAMRA, while obvious transient absorption related to the radical anion of TAMRA was not observed in the wavelength range of 350–650 nm (Figure 3A). Interestingly, the time constant of recovery of the bleach followed the similar trend with the τ-values measured for Acr^+-modified DNA (Table 1, Figure 3D). The bleach did not recover

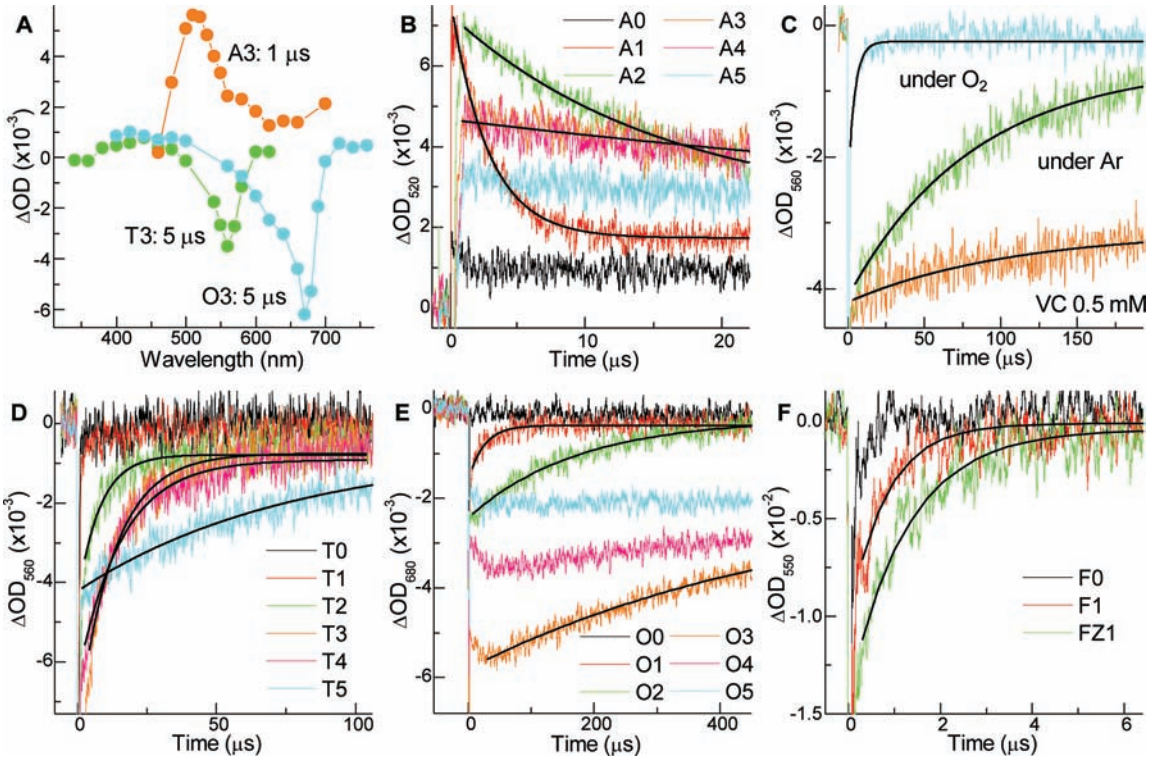

Figure 3. (A) Transient absorption spectra for **A3**, **T3**, and **O3** observed after the laser flash excitation. (B) Time profiles of the transient absorption of $PTZ^{\bullet+}$ and $Acr^{\bullet}$ monitored at 520 nm during the 355-nm laser flash photolysis of **A0**−**A5**. (C) Time profiles of the bleach and recovery of TAMRA monitored at 560 nm for **T3** under Ar, under O_2, and in the presence of 0.5 mM ascorbic acid (VC) under Ar. (D−F) Time profiles of the bleach and recovery of (D) TAMRA monitored at 560 nm for **T0**−**T5**, (E) ATTO 655 monitored at 680 nm for **O0**−**O5**, and (F) Alexa 532 monitored at 550 nm for **F0**, **F1**,, and **FZ1** during the 532-nm laser flash photolysis. The smoothed black curves superimposed on the experimental data are the single exponential fit from which the lifetime of the charge-separated state (τ) was determined. The spike near time zero is due to imperfect subtraction of the rather strong fluorescence.

Table 1. The Lifetime (τ) and Quantum Yield (Φ) of the Long-Lived Charge-Separated State

DNA	τ (μs)	Φ (%)	DNA	τ (μs)	Φ (%)	DNA	τ (μs)	Φ (%)	DNA	τ (μs)	Φ (%)
A0	<0.05	–	**T0**	<0.5[a]	–	**O0**	<0.5[a]	–	**F0**	<0.5[a]	–
A1	2.7	4.8	**T1**	<0.5[a]	–	**O1**	5.8	0.57	**F1**	0.70	1.7
A2	16	4.4	**T2**	7.6	0.36	**O2**	160	0.76			
A3	75	2.9	**T3**	13	0.61	**O3**	560	2.4			
A4	>200	2.6	**T4**	16	0.52	**O4**	>800	1.5			
A5	>200	2.0	**T5**	76	0.34	**O5**	>800	0.90			
AZ1	2.4	9.9	**TZ1**	<0.5[a]	–	**OZ1**	5.4	2.3	**F1Z**	0.96	2.6
AZ2	2.1	13	**TZ2**	<0.5[a]	–	**OZ2**	4.4	4.0			
AZ3	2.0	4.9	**TZ3**	<0.5[a]	–	**OZ3**	4.2	0.95			
AZ4	15	6.5	**TZ4**	7.7	0.43	**OZ4**	220	2.8			
AZ5	15	7.6	**TZ5**	8.1	0.51	**OZ5**	210	3.5			
AZ6	13	7.3	**TZ6**	5.7	0.51	**OZ6**	100	2.4			

[a] Though the time resolution of our experimental setup is 0.05 μs, τ shorter than 0.5 μs could not be measured for DNA **T0**, **T1**, **TZ1**−**TZ3**, **O0**, and **F0** due to the spike near time zero caused by imperfect subtraction of the rather strong fluorescence.

when the positive charge generated in DNA was reduced by ascorbic acid, and the recovery rate was increased in the presence of molecular oxygen due to the reaction of the one-electron reduced TAMRA and molecular oxygen (k_{O2} = 1.6×10^8 M^{-1} s^{-1}, Figure 3C). These results indicated that the bleaching and recovery of the ground state absorption of TAMRA corresponds to the charge-separation and -recombination dynamics in DNA.

Similarly, bleach and recovery of the ground state absorption of fluorescent dyes was investigated for ATTO 655 and Alexa 532 modified DNA. Both ATTO 655 and Alexa 532 showed sequence-dependent bleach and recovery of their ground state absorption consistent with the charge-recombination dynamics observed for Acr^+- and TAMRA-modified DNA (Table 1, Figure 3E,F). These results suggested that charge-recombination dynamics may also be monitored for other fluorescent dyes for which the

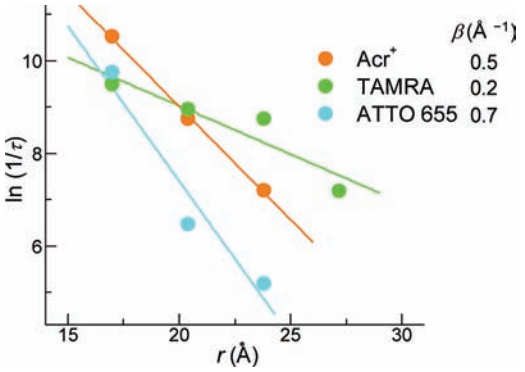

Figure 4. Distance dependence of the charge recombination rate $(1/\tau)$ through DNA. Distance between base pairs is assumed to be 3.4 Å.

fluorescence is quenched by G.[38,45] The baseline offsets tends to become larger with the increase in τ. Though these kinds of baseline offsets were often observed in the charge-separation and -recombination process in DNA having longer lifetimes,[19,20] we could not manage to identify them so far and it is the subject for future work.

The trends of the observed charge-separation, charge-migration, and charge-recombination processes varied to some extent depending on the fluorescent dye. Among the four fluorescent dyes studied here, τ-values measured for TAMRA-modified DNA were shorter and less dependent on the distance between the PTZ and the fluorescent dye compared with the corresponding sequences of the other three fluorescent dyes. The distance dependence of charge transfer is conventionally evaluated by the following eq 1,

$$1/\tau = k_0 \exp(-\beta r) \quad (1)$$

where k_0 is the preexponential factor, β is the attenuation factor of $1/\tau$, and r is the distance between PTZ and the fluorescent dye. The β-value was derived from the linear fit of the plots of $\ln(1/\tau)$ versus r (Figure 4). The β-values of 0.5 and 0.7 $Å^{-1}$ obtained for Acr^+ and ATTO 655-modified DNA, respectively, were within the range of previously reported β-values for single-step charge-transfer in DNA.[58,65−68] In contrast, the value of 0.2 $Å^{-1}$ obtained for TAMRA-modified DNA was significantly smaller than the reported β-values for the single-step charge-transfer process. Though it is well documented that the charge recombination rate is strongly affected by the driving force of the charge-recombination, which should vary for each fluorescent dye, a detailed discussion would be difficult since not all the structure and redox properties of fluorescent dyes studied here are available (the structure of ATTO 655 is proprietary).

Refinement of the Charge-Separation and Charge-Migration Processes. G's should be located close to the fluorescent dye for the photoinduced charge-transfer to efficiently occur. However, when G is located too close to the fluorescent dye, the initial charge-recombination between $G^{\bullet+}$ and the reduced fluorescent dye proceeds relatively fast compared with the charge-migration process through consecutive G's, and only part of a generated positive charge can escape from the initial charge recombination to produce a long-lived charge-separated state, thus, resulting in a moderate value of Φ.[20] To increase the Φ, we attempted to increase the rate of positive charge migration through DNA toward PTZ by replacing some G's in the G−C tract between the fluorescent dye and PTZ with Z. Since the oxidation potential of Z is lower than that of G, we expected the charge migration from $G^{\bullet+}$ to Z to proceed faster than that from $G^{\bullet+}$ to G, and at the same time that from $Z^{\bullet+}$ to G to proceed slower than that from $G^{\bullet+}$ to G, resulting in an increase in Φ.[10,69] Interestingly, for a DNA series having one A−T base-pair between the fluorescent dye and the G−C tract, the replacement of one or two G(s) with Z(s) resulted in a considerable increase in Φ (Table 1, Figure 5). On the other hand, when all G's in the G−C tract were replaced with Z, Φ was only moderately affected, suggesting that charge migration between $Z^{\bullet+}$ and Z proceeds with a similar rate constant to that between $G^{\bullet+}$ and G. In the case of DNA having two A−T base-pairs between the fluorescent dye and G−C tract, the effect of the replacement of G's with Z's on Φ was relatively small compared to those for DNA series with one A−T base-pair between the fluorescent dye and G−C tract. This result was explained by the decrease in the initial charge-recombination rate as a consequence of the increase in the distance between the fluorescent dye and the nearest G−C or Z−C. In contrast to the **YZ3** series, an increase in Φ was also observed for the **YZ6** series. While the charge-migration rate through the ZZZ sequence is comparable to that of the GGG sequence, the increase in the photoinduced charge-transfer efficiency, which is reflected in the increased extent of the florescence quenching, caused the increase in Φ.

In all cases, the substitution of GGG with ZZZ (**YZ3** and **YZ6**) resulted in a decrease of the τ. It is well-established that the energy gap between the donor and the bridge states affects the electronic coupling, that is, the electron transfer rate in the donor-bridge-acceptor system.[70−74] The replacement of G with Z having a lower oxidation potential resulted in a decrease in the energy gap and thus increased the charge-recombination rate. These results clearly showed that information about the micro-environment around the fluorescent dye can be extracted by measuring the τ.

Charge-Separation in DNA Utilizing Z as a Positive Charge Trap. We chose ATTO 655 to probe the charge-transfer dynamics in DNA at the single-molecule level, because it possesses some characteristics that make possible the FCS measurements of the charge-transfer dynamics in DNA. The very low inter-system crossing yield of ATTO 655 almost completely suppresses the formation of the nonfluorescent triplet excited states, which hamper the extraction of charge-transfer dynamics from the FCS measurements. The slow reaction rate of its radical anion with molecular oxygen allows the experiments to be carried out under aerobic conditions, which also prevent the formation of the long-lived triplet states.[42,43,47−49] Unfortunately, PTZ was unstable at low concentrations typically used in FCS measurements (<5 nM), and instead, we utilized Z as a positive charge trap (Figure 6). We replaced some A's with diaminopurines (D's), which has a higher HOMO level than A, to create a better pathway for a charge in DNA.[21,62] A−T base-pair(s) was inserted between the ATTO 655 and G or D to serve as a spacer to slow down the initial charge-recombination rate, allowing for the formation of a charge-separated state longer than 1 μs. Thus, the fluorescence intensity was only moderately affected by the sequence (Figure 7A).

Charge-recombination dynamics in the ATTO 655 and Z system were first investigated by the conventional transient absorption measurement. To measure the τ more precisely, He−Ne CW-laser (633 nm) was used as a probe light to minimize the excitation of ATTO 655 by the probe light. The 532-nm laser excitation of ATTO 655 bleached the ground state absorption of

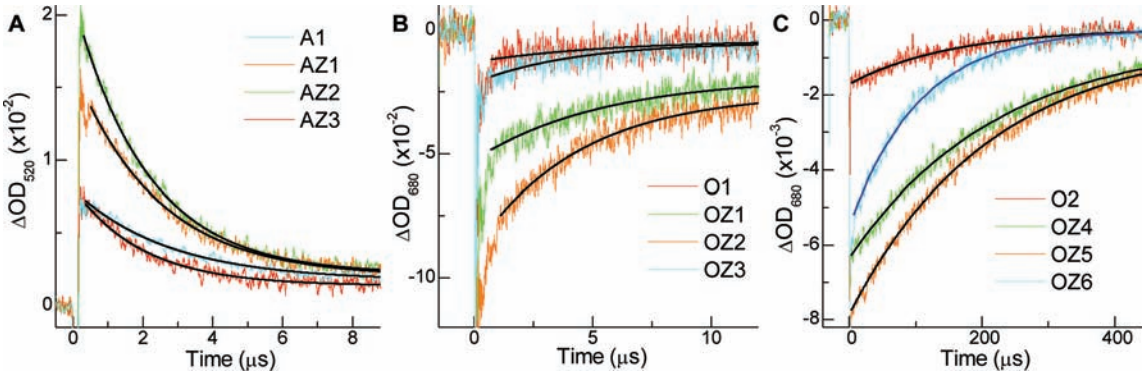

Figure 5. The effects of replacing G base(s) with Z base(s) on the charge-separation and charge-recombination dynamics in DNA. (A) Time profiles of the transient absorption of $PTZ^{\bullet+}$ and $Acr^{\bullet}$ monitored at 520 nm during the 355-nm laser flash photolysis of **A1**, and **AZ1**−**AZ3**. Time profiles of the bleach and recovery of ATTO 655 monitored at 680 nm for (B) **O1**, **OZ1**−**OZ3**, and (C) **O2**, **OZ4**−**OZ6** during the 532-nm laser flash photolysis. The smoothed black curves superimposed on the experimental data are the single exponential fit from which the lifetime of the charge separated state (τ) was determined. The spike near time zero is due to imperfect subtraction of the rather strong fluorescence.

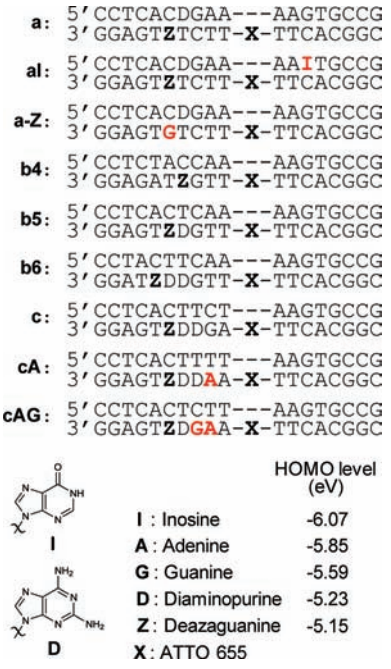

Figure 6. Sequences of DNA investigated in ATTO 665 and Z system. Some A's were replaced with diaminopurines (D's) having higher HOMO-level than A, to create a better pathway for a charge in DNA. One G was replaced with Z to serve as a charge trap. The HOMO levels of the N-methylated nucleobases are the values calculated at B3LYP/6-31G(d).

ATTO 655 and the subsequent recovery of its absorbance (Figure 7B, and Supporting Information Figure S1). The recovery rate was not affected by the dissolved molecular oxygen, thus, precluding the formation of the triplet excited state of ATTO 655, and the bleach did not recover when the positive charge generated in DNA was reduced by ascorbic acid (Supporting Information Figures S2 and S3). These results clearly showed that bleaching and recovery correspond to the charge-separation and -recombination dynamics in DNA. The replacement of the 3′ neighboring G in the top strand by inosine (I), having a lower HOMO level than G, which in turn was similar to that of A, did not affect the time profile (**aI**),[59] and the charge-separated state did not form when the charge trap Z was replaced with G (**a-Z**). This demonstrated that the observed charge-separated state is attributed to the formation of the radical anion of ATTO 655 and the radical cation of Z.

The quantum yield of the formation of the long-lived charge-separated state for **a** was measured to be 5.6% (Table 2). The initial charge-recombination between the radical anion of ATTO 655 and the radical cation of G proceeds relatively fast compared with the charge-migration process through DNA, and only part of a generated positive charge can escape from the initial charge recombination to be trapped at Z, thus, resulting in a moderate charge-separation yield similar to the ATTO 655 and PTZ system. The photoinduced charge-transfer may also proceed with the 3′ neighboring G in the top strand but charge-recombination takes place faster than the time resolution of our experimental setup (<50 ns).

Time profiles were better fitted with a double-exponential function. The relative amplitude of the slower component increased by decreasing the pH of the solution, suggesting that the slower component may be associated with the protonation process of the radical anion of ATTO 655 (Supporting Information Figure S4). A weighted average of the biexponential-decay components was used to compare the lifetime of the charge separated state measured by transient absorption with that measured by FCS.

FCS Measurement of Charge-Recombination Dynamics in DNA. Next, the charge-transfer dynamics in the ATTO 655 and Z system were probed using FCS. In addition to the diffusion component with a time constant of hundreds of microseconds, an additional relaxation process was observed in the time range of microsecond to tens of microseconds (Figure 7C, **a**). The time constant of the additional component (τ_{FCS} Figure 7A, green) correlated well with the τ measured from the transient absorption measurements (τ_{TA} Figure 7A, blue), and was attributed to the on/off dynamics of the single ATTO 655 due to the formation of the nonemissive charge-separated state in DNA. The τ_{FCS} was unaffected by the addition of 5% PEG-20,000, which increased the diffusion time constant, precluding an intermolecular reaction such as that between a molecular oxygen and a triplet excited state of ATTO 655, and also precluding the formation of a nonfluorescent complex between ATTO 655 and

dx.doi.org/10.1021/ja206325m |J. Am. Chem. Soc. 2011, 133, 15568–15577

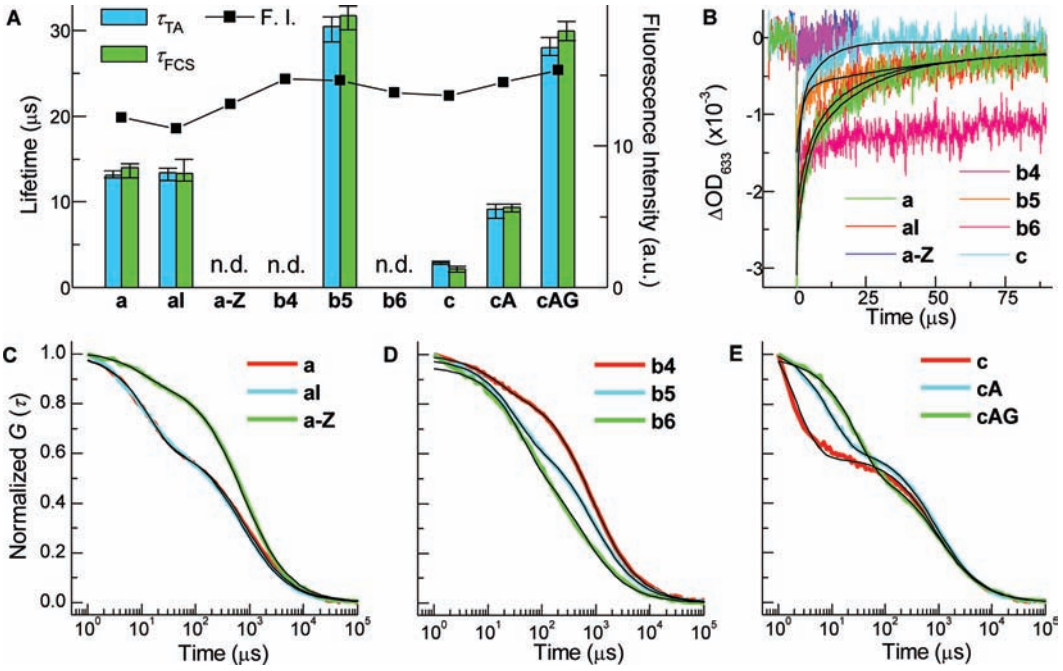

Figure 7. Charge recombination dynamics measured by transient absorption and FCS. (A) Comparison between lifetime of the charge separated state measured by transient absorption (τ_{TA}, blue bar) and by FCS (τ_{FCS}, green bar), and fluorescence intensity (λ_{ex} = 620 nm, λ_{em} = 684 nm, line plot) measured for ATTO 655 modified DNA. (B) Time profiles of the bleach and recovery of ATTO 655 monitored at 633 nm during the 532-nm laser flash photolysis of DNA **a**, **aI**, **a-Z**, **b4**, **b5**, **b6**, and **c**. The smoothed black curves superimposed on the experimental data are the double exponential fit from which the lifetime of the charge separated state (τ_{TA}) was determined. (C−E) FCS time traces for (C) **a**, **aI**, **a-Z**, (D) **b4**, **b5**, **b6**, and (E) **c**, **cA**, **cAG**. The smoothed black curves superimposed on the experimental data correspond to the theoretical fitting curves according to eq 2.

electron-donating nucleobases (G, D, or Z) (Supporting Information Figures S5 and S6).[75−77] UV Melting-temperature (T_m) measurements supported that ATTO 655 is anchored and buried in DNA to have π-stacking interaction between neighboring bases (Supporting Information Figure S7). The amplitude of the additional component increased with the applied laser intensity (Supporting Information Figure S8), and these results are all consistent with the on/off dynamics of the fluorescence from a single ATTO 655 due to the formation of the nonemissive charge-separated state in DNA.

The τ_{FCS} values determined from FCS measurements were in good accordance with the dynamics of the charge-transfer in DNA as previously reported by Lewis and Wasielewski's group[8,9,71] as well as by us.[19,21,62,78] The increasing distance between ATTO 655 and Z resulted in an exponential increase of τ_{FCS}. Charge recombination proceeds within 1 μs for **b4** due to the close distance between Z and ATTO 655, is clearly observed for **b5**, and in the case of **b6**, τ_{FCS} becomes too long and indistinguishable from the diffusion process (Figure 7D). This makes it difficult to accurately measure the τ_{FCS} and also the diffusion time constant (τ_D) (Table 2), suggesting that a longer DNA that show a longer τ_D should be targeted to access the charge-recombination dynamics in the longer time range. As mentioned above, the energy gap between the donor and the bridge states affects the electronic coupling, that is , the charge transfer rate in the donor-bridge-acceptor system.[70,71] The τ_{FCS} was affected by the bridge bases between ATTO 655 and Z, where a decrease in the HOMO level of the bridge base caused by the replacement of G to A (**c** → **cA**) and the replacement of D to G (**cA** → **cAG**) resulted in an increase in the τ_{FCS} (Figure 7E). In all cases, the τ_{FCS} (Figure 7A, green) agreed well with τ_{TA} (Figure 7B. blue), clearly showing that single base differences in DNA sequence can be probed by single-molecule-level fluorescence measurement (Table 2).

In the case of **a-Z** and **b4**, formation of the charge-separated state which does not correspond to the charge trapping at Z was observed to a minor extent in the FCS measurement due to the much higher sensitivity of FCS compared to that of transient absorption measurement. These results suggest that not only Z, but also D and/or G may serve as a charge trap to probe the charge transfer dynamics by FCS measurement.

SNP Detection. Chemical SNP typing methods often employ allele-specific oligonucleotides that hybridize to the target SNP sequence.[79−81] Hybridization of the probe oligonucleotides results in a fully matched duplex formation for the wild-type target, whereas for the SNP mutant target, a mismatched duplex forms, and thus, the detection of a mismatch allows the SNP typing. Since the presence of a mismatch causes the perturbation of the π-stacks, resulting in a decrease in charge-transfer rates,[78,81−85] we investigated the effect of a mismatch on the charge-recombination dynamics by FCS measurements. The presence of a mismatch caused significant changes in τ_{FCS} depending on the position and the type of the mismatch, and a mismatch located closer to the middle of the donor and acceptor was shown to cause a larger perturbation on the charge transfer dynamics in DNA (**c**, **m1**−**m6**, Figure 8). These results demonstrated that DNA sequence information regarding SNPs can be extracted by charge-transfer dynamics measurements at the single-molecule level by arranging the probe DNA so as to locate the SNP site in the middle of the donor and acceptor. Although the presence of a mismatch between a donor and an acceptor caused a significant decrease

in the charge separation yield, the high sensitivity of FCS techniques allowed the measurement of charge-transfer dynamics. The present method enables the automatic measurement and analysis of more than 100 samples within 2 h using less than 0.1 pmol of sample, which is over 10 000 times less than that typically required for transient absorption measurements.[8,21,71,78]

Table 2. Charge Recombination Dynamics Measured by Transient Absorption (τ_{TA}) and FCS (τ_{FCS}), Quantum Yield of the Long-Lived Charge Separated State (Φ), and the Mean Fraction of ATTO 655 within the Sample Volume Element Being in Charge-Separated State (C), and the Diffusion Time Constant (τ_D) Measured by FCS

	TA[a]			FCS[b]		
DNA	τ_{TA} (μs)		Φ (%)	τ_{FCS} (μs)	C (%)	τ_D (μs)
a	13	(3.0 (47%), 23 (53%))	5.6	14	38	860
aI	13	(3.9 (44%), 20 (56%))	4.6	13	37	740
a-Z	–	–	–	12[c]	13[c]	770
b4	<1	–	–	16[c]	15[c]	860
b5	30	(2.1 (59%), 71 (41%))	2.8	32	32	890
b6	>100	–	3.2	45[d]	39[d]	580[d]
c	2.9	(0.81 (70%), 7.8 (30%))	6.6	2.2	51	850
cA	9.2	(2.7 (55%), 17 (45%))	2.7	9.3	40	920
cAG	28	(3.9 (60%), 65 (40%))	3.6	30	47	1,000
m1	–	–		5.9	42	840
m2	–	–		6.3	54	870
m3	–	–		30	33	840
m4	–	–		11	35	810
m5	–	–		8.8	39	880
m6	–	–		3.8	38	770

[a] Determined from the nanosecond transient absorption measurements as described in the main text, Experimental Section. τ_{TA} was determined as a weighted average of the biexponential decay components. [b] Obtained from the FCS measurement using MF20 (Olympus) as described in the main text, Experimental Section. [c] Formation of the charge-separated state which does not correspond to the charge trapping at Z was observed to a minor extent in the FCS measurement due to the much higher sensitivity of FCS compared to that of transient absorption measurement. [d] Lifetime of the charge-separated state becomes too long and indistinguishable from the diffusion process, making it difficult to accurately measure both τ_{FCS} and τ_D.

CONCLUSIONS

We synthesized DNA site specifically modified with a fluorescent dye: TAMRA, ATTO 655, or Alexa 532, which are widely used in single-molecule fluorescence studies. These fluorescent dyes were demonstrated to undergo charge-separation and recombination in DNA in the time range of nanosecond to milliseconds. Charge-separation and -recombination dynamics in ATTO 655 modified DNA were clearly probed by FCS measurement at the single-molecule level. The typical quantum yield of the charge-separation process discussed in the present report is lower than 10%, showing that charge-transfer dynamics can be probed with high sensitivity by FCS even when charge separation is a rather minor photochemical process. Although the blinking of fluorescence emitted from single molecules is often attributed to the formation of the charge-separated state, the information available from the blinking was usually passed over during the live-cell imaging and diagnosis. The present report clearly demonstrated that the measurement of blinking serves as a powerful tool for extracting local information around the fluorescent dyes in addition to those accessible from the measurements of changes in the fluorescence intensities or fluorescent lifetimes. The recent advances in the FCS techniques[55−57] may open the way for the read-out of DNA and RNA sequence information in living cells. The present results have demonstrated that the charge-recombination dynamics of fluorescent dyes can be regulated in the time range of submicroseconds to milliseconds. The control of the blinking caused by the charge-separation, charge-migration, and charge-recombination may also be useful in improving super-resolution techniques, which are based on the blinking of the fluorescent dyes.[42,86−91]

EXPERIMENTAL SECTION

Synthesis of Fluorescent Dye Modified DNA. Phosphoroamidite derivative of amino linker used in this study was synthesized according to the reported procedure.[92] Phosphoroamidite derivative of Acr^+, Z, D, and all other reagents for DNA synthesis were purchased from Glen Research. DNAs were synthesized on an Applied Biosystems DNA synthesizer A3400 and purified by reverse phase HPLC and lyophilized. Fluorescent dyes other than Acr^+ were attached to DNA via the reaction of the amino-linker modified DNA using the succinimidyl derivative of TAMRA (Anaspec, Inc.), ATTO 655 (ATTO-TEC), and Alexa 532 (Invitrogen) according to the standard procedure. Briefly, *N*-succinimidyl ester derivative of fluorescent dye was incubated with an amino-linker modified DNA under pH 9.0 Na carbonate buffer at 25 °C for 12−24 h. The excess fluorescent dye was removed by spin column

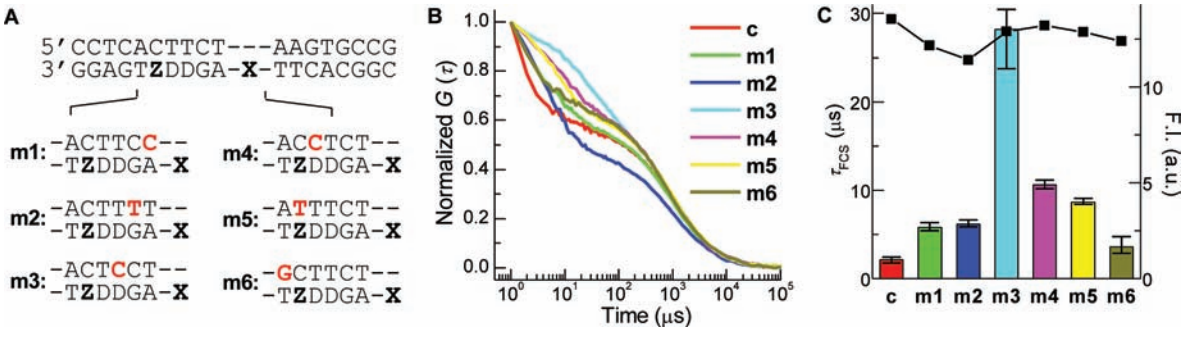

Figure 8. Detection of a mismatch by charge-transfer dynamics measurements using FCS. (A) Sequences of DNA containing a mismatch; (B) FCS time traces for **c**, and **m1**−**m6**; (C) comparison between lifetime of the charge separated state measured by FCS (τ_{FCS}) and fluorescence intensity (λ_{ex} = 620 nm, λ_{em} = 684 nm, line plot) measured for **c**, and **m1**−**m6**.

dx.doi.org/10.1021/ja206325m |*J. Am. Chem. Soc.* 2011, 133, 15568–15577

(BioRad), and fluorescent dye-modified DNA was purified using reverse-phase HPLC and characterized by MALDI-TOFF mass spectra. The incorporation yield was in the range of 20−40%, while that for Alexa 532 was less than 10%, and thus, only **F0**, **F1**, and **FZ1** were synthesized.

Transient Absorption Measurements. The nanosecond transient absorption measurements were performed using the laser flash photolysis technique for an aqueous solution of DNA (Acridine, 40 μM; TAMRA, 10 μM; ATTO 655, 7.5 μM; Alexa 532, 15 μM) containing 10 mM $MgCl_2$, 100 mM NaCl, and 10 mM pH 7.0 Na phosphate buffer in a final volume of 300 uL. The third-harmonic oscillation (355 nm, fwhm of 4 ns, 10 mJ/pulse) or the second-harmonic oscillation (532 nm, fwhm of 4 ns, 3 mJ/pulse) from a Q-switched Nd:YAG laser (Continuum, Surelight) was used for the excitation light for Acr^+, and TAMRA, ATTO 655, and Alexa 532, respectively. A xenon flash lamp (Osram, XBO-450) was focused into the sample solution as a probe light for the transient absorption measurement. He−Ne CW-laser (633 nm, Melles Griot) was used as a probe light for ATTO 655 and Z system. Time profiles of the transient absorption were measured with a monochromator (Nikon, G250) equipped with a photomultiplier (Hamamatsu Photonics, R928) and digital oscilloscope (Tektronics, TDS-580D). The time profiles were obtained from the average of 32 laser shots, and the lifetime of the charge-separated state was determined by single-exponential fitting of the data. For ATTO 655 and Z system, τ_{TA} was determined by double-exponential fitting of the data. The experiment was carried out under Ar unless otherwise mentioned.

Measurements of Quantum Yield (Φ) of Charge Separation. An CH_3CN solution of benzophenone was prepared so as to give the same absorption at 355 nm as the Acr^+- and PTZ-modified DNA solution. The Φ was determined by comparing the sum of the transient absorption of $PTZ^{\bullet+}$ (ε_{520} = 9300 M^{-1} cm^{-1})[93] and $Acr^{\bullet}$ (one-electron reduced form of Acr^+, ε_{520} = 4000 M^{-1} cm^{-1})[94] with that of benzophenone (Φ_T = 1, ε_{520} = 6500 M^{-1} cm^{-1})[95] at 520 nm upon the 355-nm laser excitation. For TAMRA, ATTO 655, and Alexa 532-modifed DNA, a toluene solution of fullerene was used to measure the Φ (Φ_T = 0.93, ε_{750} = 16 100 M^{-1} cm^{-1}).[96] The Φ was estimated by comparing the ground state bleach of TAMRA (ε_{560} = 71 500 M^{-1} cm^{-1}), ATTO 655 (ε_{680} = 69 900 M^{-1} cm^{-1}), and Alexa 532 (ε_{550} = 18 300 M^{-1} cm^{-1}) with the transient absorption of fullerene in the triplet excited state.

FCS Measurements. The FCS measurements were carried out using the MF20 (Olympus)[97] in an aqueous solution containing 2 nM of ATTO-labeled probe-strand, 4 nM of target strand, 10 mM $MgCl_2$, 100 mM NaCl, 5% PEG-20,000, and 10 mM pH 7.0 Na phosphate buffer in a final volume of 45 μL under air. He−Ne laser (633 nm, 400 μW) was used as the excitation source. All experiments were performed with 10 s of data acquisition time per measurement, and repeated five times per sample, and τ_{FCS} was determined by fitting the data using the following equation,

$$G(\tau) = 1 + \left(\frac{1}{N}\right)\left(\frac{1}{1+\tau/\tau_D}\right)\left(\frac{1}{1+(1/S^2)(\tau/\tau_D)}\right)^{1/2}\left(1+\frac{C}{1-C}\right)\exp\left(-\frac{\tau}{\tau_{FCS}}\right) \quad (2)$$

where N is the number of molecules within the sample volume element, τ_D is translational diffusion time, $S = \omega_1/\omega_0$ is radius of the measurement area ω_0 and half of its axial length ω_1, C is the mean fraction of fluorophores within the sample volume element being in the charge-separated state, and τ_{FCS} is lifetime of the charge-separated state.

■ ASSOCIATED CONTENT

Supporting Information. Supporting figures as noted in text. This material is available free of charge via the Internet at http://pubs.acs.org.

■ AUTHOR INFORMATION

Corresponding Author
kiyohiko@sanken.osaka-u.ac.jp; majima@sanken.osaka-u.ac.jp

■ ACKNOWLEDGMENT

We thank Prof. S. Sando of Kyushu University for giving the opportunity of sample preparation in his laboratory, and Dr. N. Kato of Olympus for assistance with the data analysis. This work has been partly supported by a Grant-in-Aid for Scientific Research (Project 22245022 and 21750170) from the MEXT of Japanese Government. T.M. thanks the WCU (World Class University) program through the National Research Foundation of Korea funded by the Ministry of Education, Science and Technology (R31-10035) for the support.

■ REFERENCES

(1) Doose, S.; Neuweiler, H.; Sauer, M. *ChemPhysChem* **2009**, *10*, 1389.
(2) Kikuchi, K. *Chem. Soc. Rev.* **2010**, *39*, 2048.
(3) Kobayashi, H.; Ogawa, M.; Alford, R.; Choyke, P. L.; Urano, Y. *Chem. Rev.* **2010**, *110*, 2620.
(4) Seidel, C. A. M.; Schulz, A.; Sauer, M. H. M. *J. Phys. Chem.* **1996**, *100*, 5541.
(5) Yang, W.-Y.; Breiner, B.; Kovalenko, S. V.; Ben, C.; Singh, M.; LeGrand, S. N.; Sang, Q.-X. A.; Strouse, G. F.; Copland, J. A.; Alabugin, I. V. *J. Am. Chem. Soc.* **2009**, *131*, 11458.
(6) Gray, H. B.; Winkler, J. R. *Proc. Natl. Acad. Sci. U.S.A.* **2005**, *102*, 3534.
(7) Ener, M. E.; Lee, Y.-T.; Winkler, J. R.; Gray, H. B.; Cheruzel, L. *Proc. Natl. Acad. Sci. U.S.A.* **2010**, *107*, 18783.
(8) Lewis, F. D.; Liu, X. Y.; Liu, J. Q.; Miller, S. E.; Hayes, R. T.; Wasielewski, M. R. *Nature* **2000**, *406*, 51.
(9) Lewis, F. D.; Liu, J.; Zuo, X.; Hayes, R. T.; Wasielewski, M. R. *J. Am. Chem. Soc.* **2003**, *125*, 4850.
(10) Conron, S. M. M.; Thazhathveetil, A. K.; Wasielewski, M. R.; Burin, A. L.; Lewis, F. D. *J. Am. Chem. Soc.* **2010**, *132*, 14388.
(11) Fiebig, T.; Wan, C. Z.; Kelley, S. O.; Barton, J. K.; Zewail, A. H. *Proc. Natl. Acad. Sci. U.S.A.* **1999**, *96*, 1187.
(12) Genereux, J. C.; Barton, J. K. *Chem. Rev.* **2010**, *110*, 1642.
(13) Genereux, J. C.; Boal, A. K.; Barton, J. K. *J. Am. Chem. Soc.* **2010**, *132*, 891.
(14) Nakatani, K.; Dohno, C.; Saito, I. *J. Am. Chem. Soc.* **1999**, *121*, 10854.
(15) Okamoto, A.; Tanaka, K.; Saito, I. *J. Am. Chem. Soc.* **2003**, *125*, 5066.
(16) Kanvah, S.; Joseph, J.; Schuster, G. B.; Barnett, R. N.; Cleveland, C. L.; Landman, U. *Acc. Chem. Res.* **2010**, *43*, 280.
(17) Leung, E. K. Y.; Sen, D. *Chem. Biol.* **2007**, *14*, 41.
(18) Huang, Y. C.; Sen, D. *J. Am. Chem. Soc.* **2010**, *132*, 2663.
(19) Kawai, K.; Osakada, Y.; Takada, T.; Fujitsuka, M.; Majima, T. *J. Am. Chem. Soc.* **2004**, *126*, 12843.
(20) Kawai, K.; Osakada, Y.; Fujitsuka, M.; Majima, T. *J. Phys. Chem. B* **2008**, *112*, 2144.
(21) Kawai, K.; Kodera, H.; Osakada, Y.; Majima, T. *Nat. Chem.* **2009**, *1*, 156.
(22) Yeow, E. K. L.; Melnikov, S. M.; Bell, T. D. M.; De Schryver, F. C.; Hofkens, J. *J. Phys. Chem. A* **2006**, *110*, 1726.
(23) Clifford, J. N.; Bell, T. D. M.; Tinnefeld, P.; Heilemann, M.; Melnikov, S. M.; Hotta, J.-I.; Sliwa, M.; Dedecker, P.; Sauer, M.; Hofkens, J.; Yeow, E. K. L. *J. Phys. Chem. B* **2007**, *111*, 6987.
(24) Wu, X.; Bell, T. D. M.; Yeow, E. K. L. *Angew. Chem., Int. Ed.* **2009**, *48*, 7379.
(25) Patel, S. A.; Cozzuol, M.; Hales, J. M.; Richards, C. I.; Sartin, M.; Hsiang, J.-C.; Vosch, T.; Perry, J. W.; Dickson, R. M. *J. Phys. Chem. C* **2009**, *113*, 20264.

(26) Wang, Y.; Wang, X.; Lu, H. P. *J. Am. Chem. Soc.* **2009**, *131*, 9020.
(27) Wang, Y.; Wang, X.; Ghosh, S. K.; Lu, H. P. *J. Am. Chem. Soc.* **2009**, *131*, 1479.
(28) Hamada, M.; Nakanishi, S.; Itoh, T.; Ishikawa, M.; Biju, V. *ACS Nano* **2010**, *4*, 4445.
(29) Cordes, T.; Vogelsang, J.; Anaya, M.; Spagnuolo, C.; Gietl, A.; Summerer, W.; Herrmann, A.; Muellen, K.; Tinnefeld, P. *J. Am. Chem. Soc.* **2010**, *132*, 2404.
(30) Campos, L. A.; Liu, J.; Wang, X.; Ramanathan, R.; English, D. S.; Munoz, V. *Nat. Methods* **2010**, *8*, 143.
(31) Roy, R.; Hohng, S.; Ha, T. *Nat. Methods* **2008**, *5*, 507.
(32) Steenken, S.; Jovanovic, S. V. *J. Am. Chem. Soc.* **1997**, *119*, 617.
(33) Dohno, C.; Saito, I. In *Charge Transfer in DNA*; Wagenknecht, H.-A., Ed.; Wiley-VCH: Weinheim, 2005; p 153.
(34) Davis, W. B.; Hess, S.; Naydenova, I.; Haselsberger, R.; Ogrodnik, A.; Newton, M. D.; Michel-Beyerle, M.-E. *J. Am. Chem. Soc.* **2002**, *124*, 2422.
(35) Hess, S.; Goetz, M.; Davis, W. B.; Michel-Beyerle, M.-E. *J. Am. Chem. Soc.* **2001**, *123*, 10046.
(36) Fukui, K.; Tanaka, K.; Fujitsuka, M.; Watanabe, A.; Ito, O. *J. Photochem. Photobiol., B* **1999**, *50*, 18.
(37) Fukui, K.; Tanaka, K. *Angew. Chem., Int. Ed.* **1998**, *37*, 158.
(38) Torimura, M.; Kurata, S.; Yamada, K.; Yokomaku, T.; Kamagata, Y.; Kanagawa, T.; Kurane, R. *Anal. Sci.* **2001**, *17*, 155.
(39) Okamoto, A.; Tanaka, K.; Saito, I. *J. Am. Chem. Soc.* **2004**, *126*, 416.
(40) Takada, T.; Fujitsuka, M.; Majima, T. *Proc. Natl. Acad. Sci. U.S. A.* **2007**, *104*, 11179.
(41) Suzuki, M.; Husimi, Y.; Komatsu, H.; Suzuki, K.; Douglas, K. T. *J. Am. Chem. Soc.* **2008**, *130*, 5720.
(42) Vogelsang, J.; Cordes, T.; Forthmann, C.; Steinhauer, C.; Tinnefeld, P. *Proc. Natl. Acad. Sci. U.S.A.* **2009**, *106*, 8107.
(43) Cordes, T.; Vogelsang, J.; Tinnefeld, P. *J. Am. Chem. Soc.* **2009**, *131*, 5018.
(44) Mueller, S.; Kumari, S.; Rodriguez, R.; Balasubramanian, S. *Nat. Chem.* **2010**, *2*, 1095.
(45) Marras, S. A. E.; Kramer, F. R.; Tyagi, S. *Nucleic Acids Res.* **2002**, *30*, e122/1.
(46) Kajino, M.; Fujimoto, K.; Inouye, M. *J. Am. Chem. Soc.* **2011**, *133*, 656.
(47) Buschmann, V.; Weston, K. D.; Sauer, M. *Bioconjugate Chem.* **2003**, *14*, 195.
(48) Vogelsang, J.; Kasper, R.; Steinhauer, C.; Person, B.; Heilemann, M.; Sauer, M.; Tinnefeld, P. *Angew. Chem., Int. Ed.* **2008**, *47*, 5465.
(49) Vogelsang, J.; Cordes, T.; Tinnefeld, P. *Photochem. Photobiol. Sci.* **2009**, *8*, 486.
(50) Kinjo, M.; Rigler, R. *Nucleic Acids Res.* **1995**, *23*, 1795.
(51) Haupts, U.; Maiti, S.; Schwille, P.; Webb, W. W. *Proc. Natl. Acad. Sci. U.S.A.* **1998**, *95*, 13573.
(52) Al-Soufi, W.; Reija, B.; Novo, M.; Felekyan, S.; Kuehnemuth, R.; Seidel, C. A. M. *J. Am. Chem. Soc.* **2005**, *127*, 8775.
(53) Gansen, A.; Valeri, A.; Hauger, F.; Felekyan, S.; Kalinin, S.; Toth, K.; Langowski, J.; Seidel, C. A. M. *Proc. Natl. Acad. Sci. U.S.A.* **2009**, *106*, 15308.
(54) Kawai, T.; Yoshihara, S.; Iwata, Y.; Fukaminato, T.; Irie, M. *ChemPhysChem* **2004**, *5*, 1606.
(55) Ohsugi, Y.; Saito, K.; Tamura, M.; Kinjo, M. *Biophys. J.* **2006**, *91*, 3456.
(56) Ries, J.; Yu, S. R.; Burkhardt, M.; Brand, M.; Schwille, P. *Nat. Methods* **2009**, *6*, 643.
(57) Vukojevic, V.; Papadopoulos, D. K.; Terenius, L.; Gehring, W. J.; Rigler, R. *Proc. Natl. Acad. Sci. U.S.A.* **2010**, *107*, 4093.
(58) Lewis, F. D.; Wu, T. F.; Zhang, Y. F.; Letsinger, R. L.; Greenfield, S. R.; Wasielewski, M. R. *Science* **1997**, *277*, 673.
(59) Kelley, S. O.; Barton, J. K. *Science* **1999**, *283*, 375.
(60) Tierney, M. T.; Sykora, M.; Khan, S. I.; Grinstaff, M. W. *J. Phys. Chem. B* **2000**, *104*, 7574.
(61) Nakatani, K.; Dohno, C.; Saito, I. *J. Am. Chem. Soc.* **2000**, *122*, 5893.
(62) Kawai, K.; Kodera, H.; Majima, T. *J. Am. Chem. Soc.* **2010**, *132*, 14216.
(63) Xiao, S. J.; Hu, P. P.; Li, Y. F.; Huang, C. Z.; Huang, T.; Xiao, G. F. *Talanta* **2009**, *79*, 1283.
(64) Seelig, J.; Leslie, K.; Renn, A.; Kuehn, S.; Jacobsen, V.; Van de Corput, M.; Wyman, C.; Sandoghdar, V. *Nano Lett.* **2007**, *7*, 685.
(65) Lewis, F. D.; Wu, Y.; Hayes, R. T.; Wasielewski, M. R. *Angew. Chem., Int. Ed.* **2002**, *41*, 3485.
(66) Wan, C. Z.; Fiebig, T.; Schiemann, O.; Barton, J. K.; Zewail, A. H. *Proc. Natl. Acad. Sci. U.S.A.* **2000**, *97*, 14052.
(67) Kawai, K.; Takada, T.; Tojo, S.; Ichinose, N.; Majima, T. *J. Am. Chem. Soc.* **2001**, *123*, 12688.
(68) Takada, T.; Kawai, K.; Fujitsuka, M.; Majima, T. *Chem.—Eur. J.* **2005**, *11*, 3835.
(69) Kawai, K.; Osakada, Y.; Fujitsuka, M.; Majima, T. *Chem.—Eur. J.* **2008**, *14*, 3721.
(70) Bixon, M.; Jortner, J. *J. Am. Chem. Soc.* **2001**, *123*, 12556.
(71) Lewis, F. D.; Liu, J.; Weigel, W.; Rettig, W.; Kurnikov, I. V.; Beratan, D. N. *Proc. Natl. Acad. Sci. U.S.A.* **2002**, *99*, 12536.
(72) Wenger, O. S.; Leigh, B. S.; Villahermosa, R. M.; Gray, H. B.; Winkler, J. R. *Science* **2005**, *307*, 99.
(73) Albinsson, B.; Martensson, J. *J. Photochem. Photobiol., C* **2008**, *9*, 138.
(74) Wenger, O. S. *Acc. Chem. Res.* **2010**, *44*, 25.
(75) Kim, J.; Doose, S.; Neuweiler, H.; Sauer, M. *Nucleic Acids Res.* **2006**, *34*, 2516.
(76) Schuettpelz, M.; Schoening, J. C.; Doose, S.; Neuweiler, H.; Peters, E.; Staiger, D.; Sauer, M. *J. Am. Chem. Soc.* **2008**, *130*, 9507.
(77) Kaji, T.; Ito, S.; Iwai, S.; Miyasaka, H. *J. Phys. Chem. B* **2009**, *113*, 13917.
(78) Osakada, Y.; Kawai, K.; Fujitsuka, M.; Majima, T. *Nucleic Acids Res.* **2008**, *36*, 5562.
(79) Nakatani, K.; Sando, S.; Saito, I. *Nat. Biotechnol.* **2001**, *19*, 51.
(80) Kim, W. J.; Sato, Y.; Akaike, T.; Maruyama, A. *Nat. Mater.* **2003**, *2*, 815.
(81) Boon, E. M.; Ceres, D. M.; Drummond, T. G.; Hill, M. G.; Barton, J. K. *Nat. Biotechnol.* **2000**, *18*, 1096.
(82) Giese, B.; Wessely, S. *Angew. Chem., Int. Ed.* **2000**, *39*, 3490.
(83) Schlientz, N. W.; Schuster, G. B. *J. Am. Chem. Soc.* **2003**, *125*, 15732.
(84) Okamoto, A.; Kamei, T.; Saito, I. *J. Am. Chem. Soc.* **2006**, *128*, 658.
(85) Slinker, J. D.; Muren, N. B.; Renfrew, S. E.; Barton, J. K. *Nat. Chem.* **2011**, *3*, 230.
(86) Steinhauer, C.; Forthmann, C.; Vogelsang, J.; Tinnefeld, P. *J. Am. Chem. Soc.* **2008**, *130*, 16840.
(87) Steinhauer, C.; Jungmann, R.; Sobey, T. L.; Simmel, F. C.; Tinnefeld, P. *Angew. Chem., Int. Ed.* **2009**, *48*, 8870.
(88) Dertinger, T.; Colyer, R.; Iyer, G.; Weiss, S.; Enderlein, J. *Proc. Natl. Acad. Sci. U.S.A.* **2009**, *106*, 22287.
(89) Vogelsang, J.; Steinhauer, C.; Forthmann, C.; Stein, I. H.; Person-Skegro, B.; Cordes, T.; Tinnefeld, P. *ChemPhysChem* **2010**, *11*, 2475.
(90) Flors, C. *Photochem. Photobiol. Sci.* **2010**, *9*, 643.
(91) van de Linde, S.; Krstic, I.; Prisner, T.; Doose, S.; Heilemann, M.; Sauer, M. *Photochem. Photobiol. Sci.* **2011**, *10*, 499.
(92) Nelson, P. S.; Kent, M.; Muthini, S. *Nucleic Acids Res.* **1992**, *20*, 6253.
(93) Alkaitis, S. A.; Beck, G.; Gratzel, M. *J. Am. Chem. Soc.* **1975**, *97*, 5723.
(94) Neta, P. *J. Phys. Chem.* **1979**, *83*, 3096.
(95) Carmichael, I.; Hug, G. L. *J. Phys. Chem. Ref. Data* **1986**, *15*, 1.
(96) Biczok, L.; Linschitz, H.; Walter, R. I. *Chem. Phys. Lett.* **1992**, *195*, 339.
(97) Choi, S. W.; Kano, A.; Maruyama, A. *Nucleic Acids Res.* **2008**, *36*, 342.